Neuron, Volume *74*

Supplemental Information

Whole-Brain Mapping of Direct Inputs to Midbrain Dopamine Neurons

Mitsuko Watabe-Uchida, Lisa Zhu, Sachie K. Ogawa, Archana Vamanrao, and Naoshige Uchida

INVENTORY OF SUPPLEMENTAL INFORMATION

Figure S1 (injection sites) is related to Figure 1

Figure S2 (cell counts from individual animals) is related to Figure 3

Figure S3 (control injections) is related to Figure 4

Figure S4 (anterograde labeling from the motor cortex) is related to Figure 5

Figure S5 (location of the ventral patches) is related to Figure 7

Figure S6 (other major input areas) is related to Figure 8

SUPPLEMENTAL FIGURES

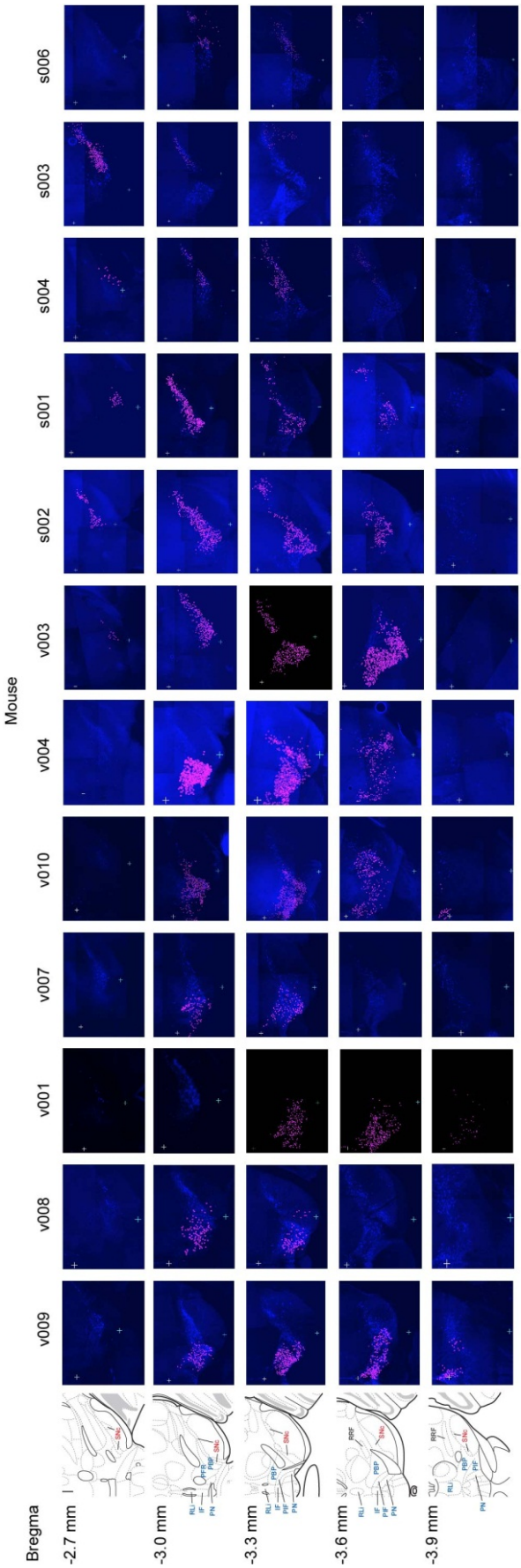

Figure S1. Distribution of starter neurons

Starter neurons (magenta) are plotted on five coronal sections. Sections were immunostained for TH (blue) except for v001. The reference atlas (Left) is from Franklin and Paxinos (2008). White crosses, midline. Cyan crosses,1 mm lateral to midline.

IF: interfascicular nucleus, PBP: parabrachial pigmented nucleus of VTA, PFR: parafasciclus retroflexus area, PIF: parainterfascicular nucleus of VTA, PN: paranigral nucleus of VTA, RLi: rostral linear nucleus, RRF: retrorubral field (A8).

Note that the IF, PBP, PFR, PIF, PN and RLi constitute the VTA or A10 (Ikemoto, 2007). In Franklin and Paxinos (2008), the VTA refers to PFR only.

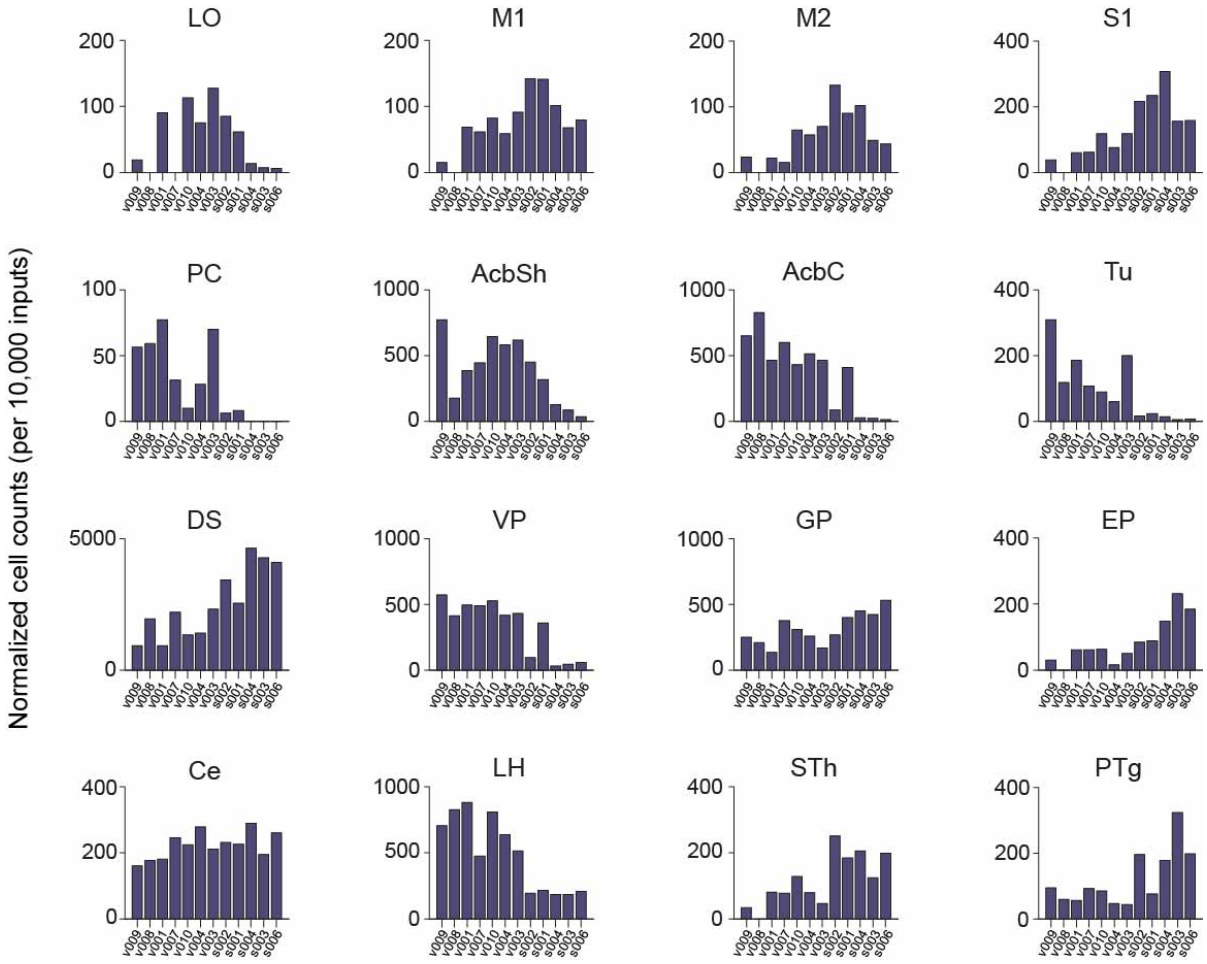

Figure S2. Cell counts from individual animals

LO, lateral orbital cortex; M1, primary motor cortex; M2, secondary motor cortex; S1, primary somatosensory cortex; PC, piriform cortex; AcbSh, nucleus accumbens shell; AcbC, nucleus accumbens core; Tu, olfactory tubercle; DS, dorsal striatum; VP, ventral pallidum; GP, globus pallidus; EP, entopeduncular nucleus; Ce, central nucleus of the amygdala; LH, lateral hypothalamus; STh, subthalamic nucleus; PTg, pedunculotegmental nucleus.

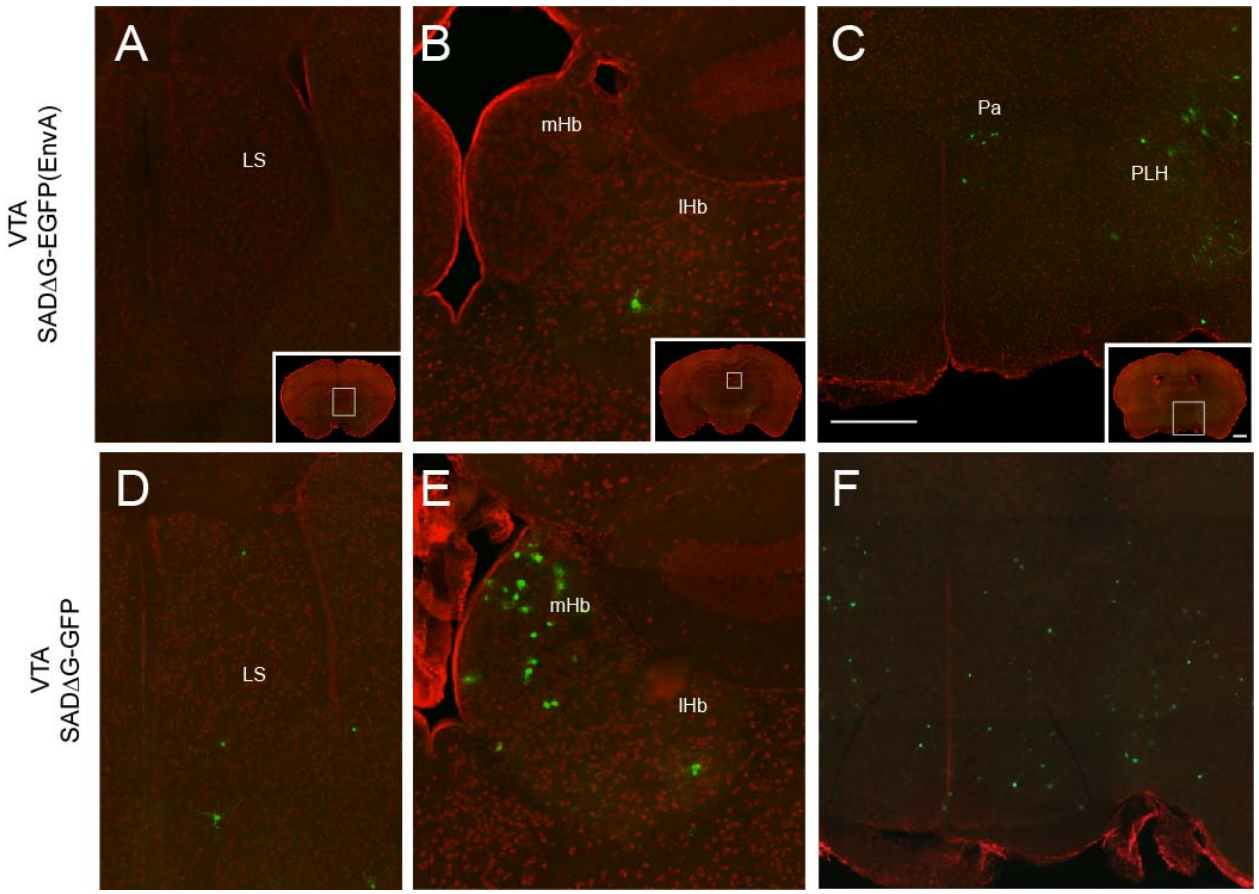

Figure S3. Comparison between tracing using Cre-dependent, transsynaptic tracing and Cre-independent, non-transsynaptic tracing.

(A, D) Lateral septum (LS)

(B, E) Medial and lateral habenula (mHb and lHb).

(C, F) Hypothalamic areas. Pa, paraventricular hypothalamic nucleus; PLH, peduncular part of the lateral hypothalamus (LH).

The EGFP patterns with selective tracing using SADdG-GFP(envA) in DAT-Cre mice (A-C) are compared with those with nonselective tracing using unpseudotyped SADdG-GFP (D-F). Green, EGFP expressed by rabies virus; red, fluorescent Nissl staining. Insets show low magnification views of sections. The white rectangles indicate the magnified regions. Scale bars, 250 μm and 1 mm (insets). Significantly more labeling is observed with nonspecific tracing in LS (D) and mHb (E) compared to the tracing with DAT-Cre mice. In the hypothalamus, Pa and LH showed prominent labeling with DAT-Cre mice (C) while more widespread labeling was observed with nonspecific tracing (F).

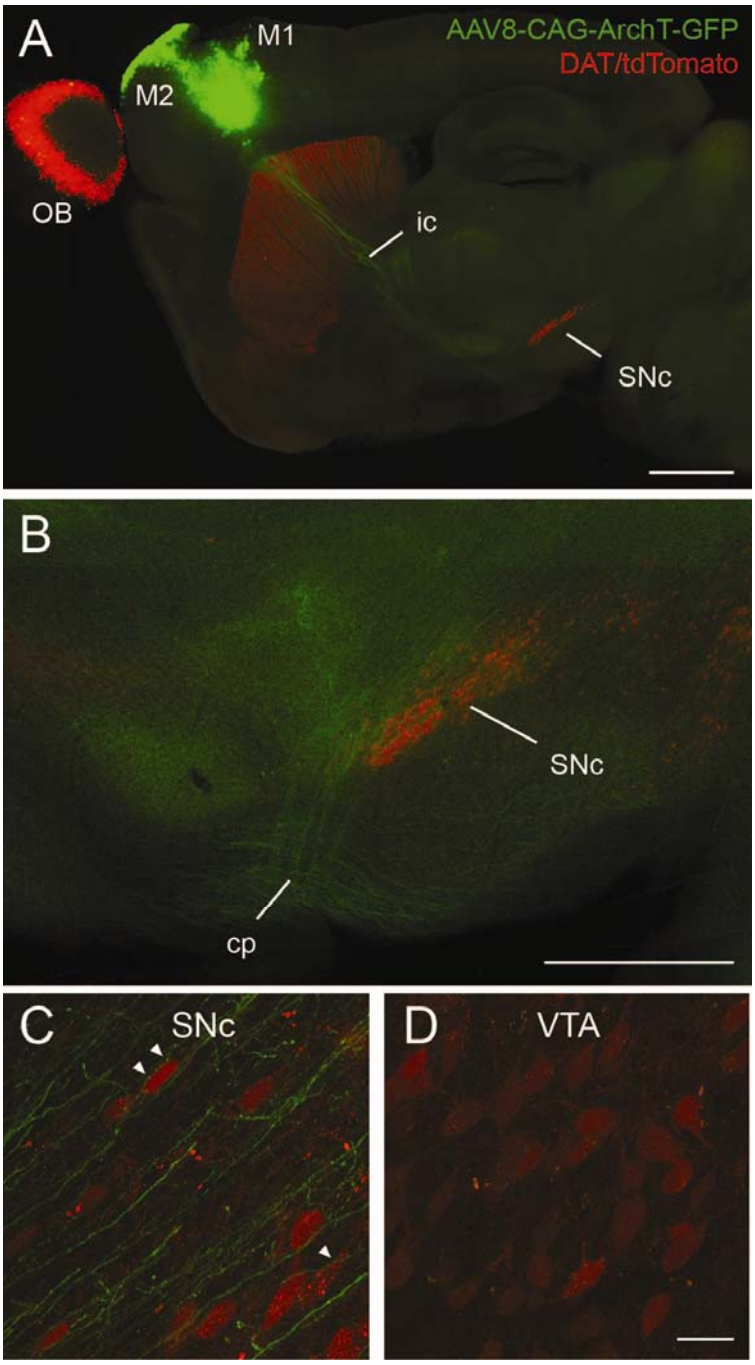

Figure S4. Anterograde tracing from the motor cortex.

(A) A low magnification view of a sagittal section. AAV8-CAG-ArchT-GFP was injected into the motor cortex. The mouse expresses tdTomato in dopamine neurons. Green: AAV8-CAG-ArchT-GFP. Red: tdTomato. Strong signals in the olfactory bulb (OB) reflect dopaminergic interneurons. Scales bar: 1 mm.

(B) A medium magnification view near SNc. Scale bar: 500 μm.

(C) A high magnification view of SNc. Arrowheads indicate buttons.

(D) A high magnification view of VTA. Scale bar: 20 μm.

cp: cortical peduncle. ic: internal capusule. OB: olfactory bulb. M1: primary motor cortex. M2: secondary motor cortex.

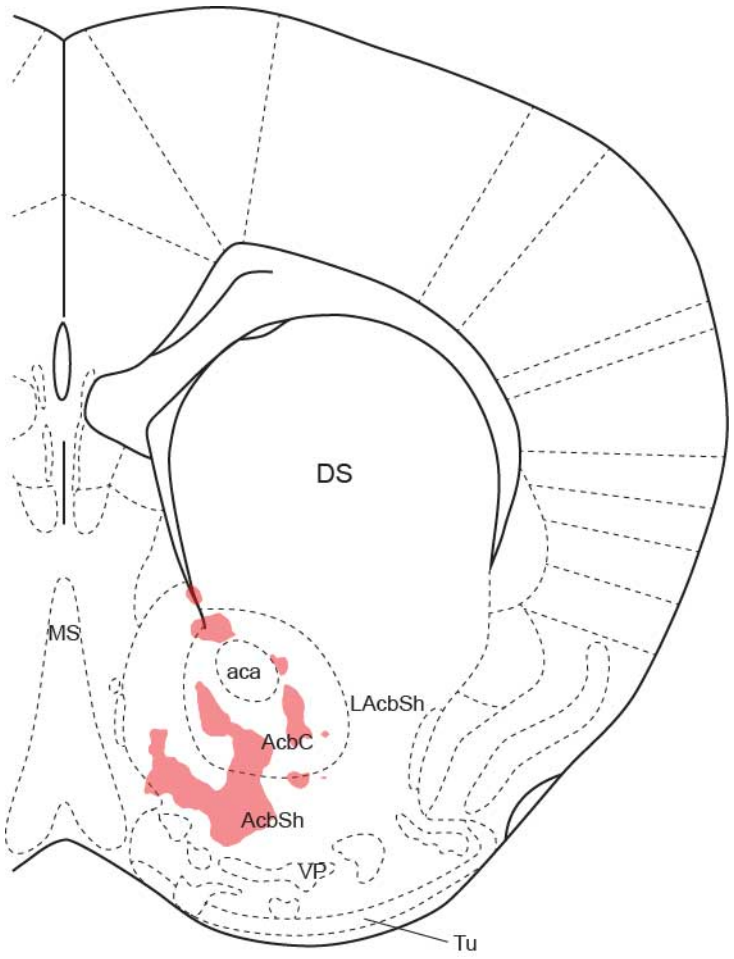

Figure S5. Patterns of dopamine neuron-projecting "ventral patches" in the nucleus accumbens.

The average patch patterns are obtained from 5 VTA-targeted mice. The atlas is after Franklin and Paxinos (2008). MS, medial septal nucleus; aca, anterior part of anterior commissure; AcbC, nucleus accumbens core; AcbSh, nucleus accumbens shell; LAcbSh, lateral accumbens shell; DS, dorsal striatum; VP, ventral pallidum; Tu, olfactory tubercle.

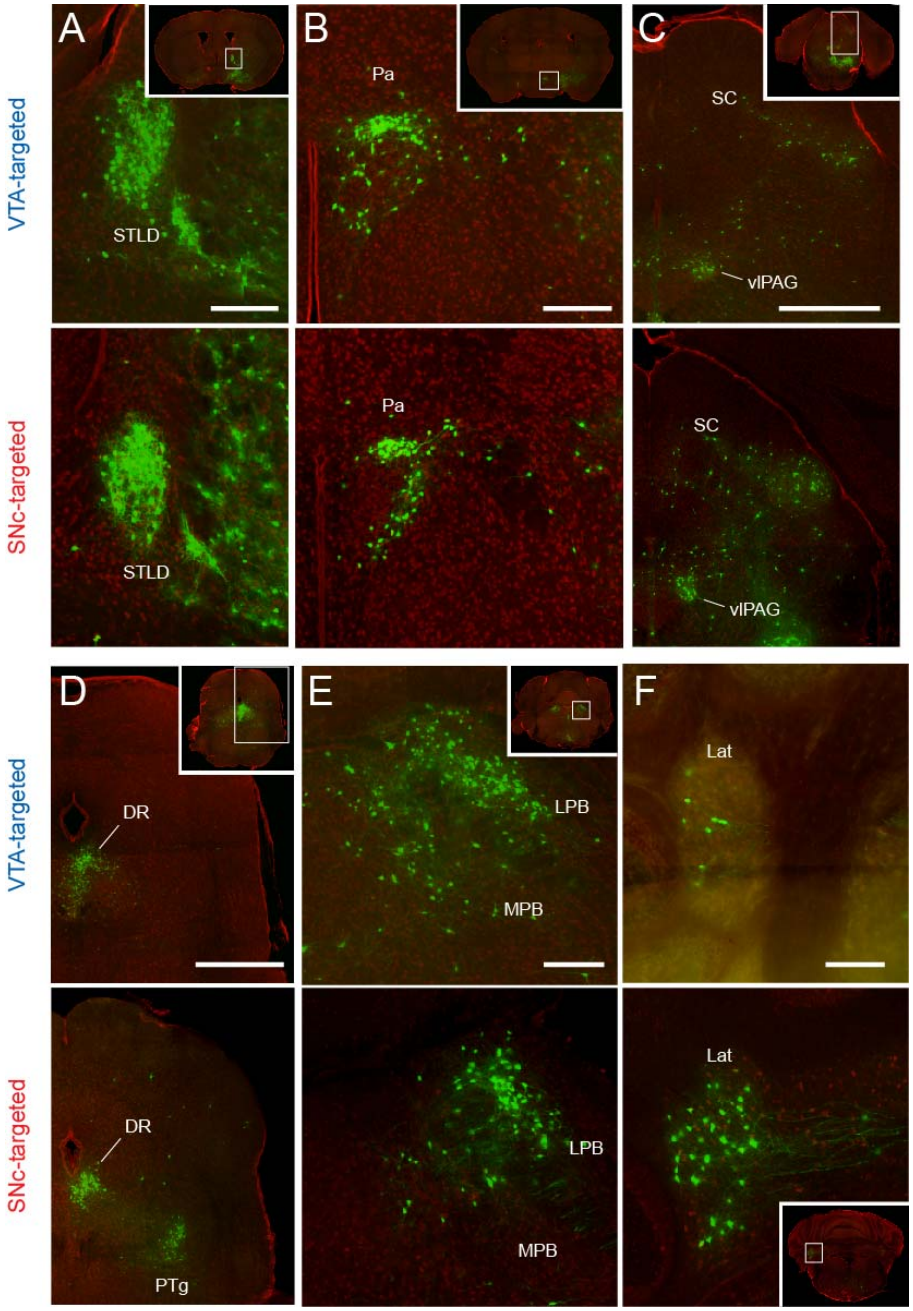

Figure S6. Comparisons of other major input areas

(A) Bed nucleus of stria terminalis (BNST). STLD, dorsal lateral division of the bed nucleus of stria terminalis.

(B) Paraventricular hypothalamic nucleus (Pa).

(C) Superior colliculus (SC) and periaqueductal gray (PAG). Dopamine projecting neurons are clustered in the ventrolateral part of the PAG (vlPAG).

(D) Dorsal raphe (DR) and pedunculotegmental nucleus (PTg).

(E) Parabrachial nucleus (PB). Both lateral and medial PB contains labeled neurons.

(F) Cerebellar nuclei. Lat, lateral (dentate) cerebellar nucleus.

Insets show low magnification views of sections. The white rectangles indicate the magnified regions. Scale bar, 1 mm (C, D) and 250 μm (A, B, E, F).

SUPPLEMENTAL EXPERIMENTAL PROCEDURES

Production of viral vectors

Different serotypes of AAVs and different promoters were used to express RG and TVA under the control of a FLEX switch (Atasoy et al., 2008), to avoid any possible competition. AAV8 and AAV5 were chosen due to the highest expression efficiency in midbrain dopamine neurons in the pilot experiments. To maximize the expression efficiency after Cre recombination, a FLEX switch was designed to contain lox2272 and loxP sites, oriented to have no false ATG start, with point mutations in the inverted repeats to destabilize hairpin structures in transcribed RNA as below. To generate a mammalian expression vector with the FLEX switch under chicken actin promoter, annealed oligonucleotides (Integrated DNA Technologies, Coralville, IA) were ligated between EcoRI and NheI sites of pCA-MCS (pCA-FLEX). CA-FLEX fragment, digested with SmaI and NheI and blunted by T4 DNA polymerase, was inserted at HindIII site, blunted and BamHI site into pAAV-DIO-hChR2EYFP (pAAV-CA-FLEX) (Gunaydin et al., 2010). Rabies glycoprotein ORF was obtained from pHCMV-RG (Sena-Esteves et al., 2004) by AseI/EcoRV digestion, blunted, and inserted at EcoRV site of pAAV-CA-FLEX (pAAV-CA-FLEX-RG).

FLEX:

GAATTCATtACcTCGTATAGGATACTTTATACGAAGTTATGCAGAATGGTAGCTGGATTGTAAGTACTA
TTAGCAATATGAAACCTCTTAATAACcTCGTATAGCATACATTATACGAAGTaATAGATCTAAGCTTGA
TATCGTCGACATAACTTCGTATAAAGTATCCTATACGAgGTaATTTGCCTTAACCCAGAAATTATCAGT
ACTATTCTTTAGAATGGTGCAAAGAATtACTTCGTATAATGTATGCTATACGAgGTTATCGCATGCTAG
C

A transmembrane version of TVA, TVA950 (Qin and Luo, 2009), was shuttled from pCMMP-TVA950 by PmlI/BamHI digestion at BamHI and EcoRV sites of pBluescriptII SK (pB-TVA950). mCherry open reading frame was amplified by PCR using pCDNA-mCherry and primers below, and inserted at StyI site blunted, and BamHI site of pB-TVA950 (pB-TVA950-mCherry). TVA950-mCherry fragment, digested with SalI and EcoRV and blunted, was inserted at NheI and AscI sites, blunted, of pAAV-DIO-hChR2EYFP (pAAV-EF1α-FLEX-TVA-mCherry).

mCherry-s: TTTTT CCC GGG GGT GGG GTG AGC AAG GGC GAG GAG G

mCherry-a: TTTTT GGATCC GAT ATC TTA CTT GTA CAG CTC GTC CA

AAV8-FLEX-RG and AAV5-FLEX-TVA-mCherry were produced by Virus Vector Core Facility of the University of North Carolina (Chapel Hill, NC). Pseudotyped and unpseudotyped rabies viruses were produced as described previously (Wickersham et al., 2010). Contamination of unpseudotyped virus was <1 in 10^4 pseudotyped virus using 293T cells.

Image analysis

The locations of labeled neurons and the outlines of brain areas were manually registered using custom software written in MATLAB (Mathworks, Natic, MA). In some cases, images were low-pass filtered using a Gaussian kernel before analysis. This reduced diffuse fluorescent signals originating from axon fibers and emphasized signals from somata. The nomenclatures and outlines of brain areas are according to a standard mouse atlas (Franklin and Paxinos, 2008). Abbreviations are also according to Franklin and Paxinos (2008) except we used the dorsal striatum (DS) instead of caudate/putamen (CPu). Note that the pedunculotegmental nucleus (PTg) is often called the pedunculopontine tegmental nucleus, and that the orbital cortex is often called the orbitofrontal cortex in other literature. The globus pallidus and entopeduncular nucleus in rodents are thought to be equivalent to the external segments and internal segments of the globus pallidus in primates, respectively. Numbers of neurons were normalized by the total number of input neurons in the entire brain of each animal. Because the numbers of input neurons are roughly proportional to those of starter neurons, both produce similar results. Because v008 and v007 contained relatively small numbers of transsynaptically labeled neurons (Figure 1F), the results from these mice were excluded from quantitative analysis. However, except some areas that contained a small number of input neurons, the results from these mice were consistent with other animals (Figure S2).

Center of mass analysis

To compare global shift of EGFP-positive neurons, the center of mass of a brain section was obtained by averaging positions of neurons. To superimpose results from different animals onto a standard atlas, neuron's positions were normalized by anatomical landmarks. For Figure 4A-C, we used the midline and the lateral most part of the dorsal striatum (DS). For Figure 4D-F, we used the midline and the medial most position of the cerebral peduncle (cp).

Analysis of the neocortex

Various efforts have been made to identify cortical areas in rodents. However, resulting maps differ significantly across studies (Plalomero-Gallagher and Zilles, 2004). We therefore examined distributions of the labeled neurons in the entire neocortex using an "unrolled map". To make an unrolled map, we first drew a line running at the middle of the cortical sheet (the gray lines in Figure 5C and F). For reference points, we used the most dorsomedial corner of the hemisphere (the black crosses in Figure 5C and F) and rhenal fissure or sulcus (red triangles). These reference points were projected onto the line (black dots and red crosses). These lines were "unrolled" and aligned according to the dorsomedial reference point and the rostro-caudal position in reference to the bregma (Figure 5G and H). This unrolled map allows one to compare results across studies independent from the discrepancies in cortical maps. For comparison, we generated a reference unrolled map according to a mouse standard atlas (Figure 5I) (Franklin and Paxinos, 2008).

For cell counting (Figure 3), areas in the neocortex were parceled mostly according to the proportions of cortical areas on the coronal slices in the standard atlas (Franklin and Paxinos, 2008). Slight changes in the locations of the boundaries of cortical areas do not significantly affect the results.

Analysis of striatal neurons

For the quantification of calbindin D-28k immunofluorescence, we normalized the pixel intensities by the maximum and minimum of the area of interest. For each neuron, intensities were obtained in a circular area with diameter 6.8 μm. For measuring soma sizes, a stack of confocal images was projected along the z-axis. The soma of each neuron was outlined using custom software written in MATLAB and the area within the contour was calculated. We then calculated the diameter based on the area assuming a circle.

For a measure of dendritic complexities (Figure 6K), dendrites were traced using custom software in MATLAB. Dendritic length is defined as the total length along the dendrite. Radial distance is defined as the straight line distance between the most proximal point of the dendrite and the tip of the dendrite.

To obtain standard "ventral patches", locations of labeled neurons from 5 VTA-targeted mice were pooled. The data from different animals were combined using a normalized coordinate using the midline and the anterior commissure (the cross in Figure 7) as the reference points. The information about the locations of labeled neurons was "smoothed" by a circular averaging filter of the radius of 0.08 mm to obtain a density map. A contour line was drawn at half of the maximum density. To test the conservation of the location of the patches, "predicted" contour maps were obtained for each animal using data from the other 4 animals (one-leave-out cross-validation method) and the proportion of the neurons within the contour lines (patches) against the total number in Acb was calculated ("% neurons in predicted contours"). We then tested whether this value is larger than the proportion of the areas of the patches compared to that of the Acb (paired t-test).

Anterograde labeling from the motor cortex

To confirm projections from the motor cortex to SNc dopamine neurons, AAV8-CAG-ArchT-GFP (1.3×10^{11} particles/ml, a gift from Dr. Edward Boyden, generated by UNC Virus Vector Core Facility, Chapel Hill, NC) was injected into the motor cortex (bregma: +2.0 mm, 1.3 mm lateral from the midline) in two mice. We used DAT-Cre/Gt(ROSA)26 $^{Sortm(CAG-tdTomato)Hze}$ (Jackson Lab, Bar Harbor, ME) to label dopamine neurons with a fluorescent marker, tdTomato. After 17 days from injection, mice were perfused with 4% paraformaldehyde, and 100 μm sagittal sections were cut for observation (Figure S4).

SUPPLEMENTAL REFERENCES

Atasoy, D., Aponte, Y., Su, H.H., and Sternson, S.M. (2008). A FLEX switch targets Channelrhodopsin-2 to multiple cell types for imaging and long-range circuit mapping. J Neurosci *28*, 7025-7030.

Franklin, B.J., and Paxinos, G. (2008). The mouse brain in stereotaxic coordinates. Compact third eddition. (San Diego, Academic Press).

Gunaydin, L.A., Yizhar, O., Berndt, A., Sohal, V.S., Deisseroth, K., and Hegemann, P. (2010). Ultrafast optogenetic control. Nat Neurosci *13*, 387-392.

Plalomero-Gallagher, N., and Zilles, K. (2004). Isocortex. In The rat nervous system, Third edition, G. Paxinos, ed. (San Diego, Academic Press), pp. 729-757.

Qin, C., and Luo, M. (2009). Neurochemical phenotypes of the afferent and efferent projections of the mouse medial habenula. Neuroscience *161*, 827-837.

Sena-Esteves, M., Tebbets, J.C., Steffens, S., Crombleholme, T., and Flake, A.W. (2004). Optimized large-scale production of high titer lentivirus vector pseudotypes. J Virol Methods *122*, 131-139.

Wickersham, I.R., Sullivan, H.A., and Seung, H.S. (2010). Production of glycoprotein-deleted rabies viruses for monosynaptic tracing and high-level gene expression in neurons. Nat Protoc *5*, 595-606.